IEEE Access
Multidisciplinary | Rapid Review | Open Access Journal

Received January 19, 2021, accepted January 23, 2021, date of publication February 2, 2021, date of current version February 11, 2021.

Digital Object Identifier 10.1109/ACCESS.2021.3056619

Common Spatial Pattern Technique With EEG Signals for Diagnosis of Autism and Epilepsy Disorders

FAHD A. ALTURKI, MAJID ALJALAL, AKRAM M. ABDURRAQEEB, KHALIL ALSHARABI, AND ABDULLRAHMAN A. AL-SHAMMA'A

Department of Electrical Engineering, King Saud University, Riyadh 11421, Saudi Arabia

Corresponding author: Majid Aljalal (algalalmajid@hotmail.com)

This work was supported by the Deanship of Scientific Research at King Saud University through research under Grant RG-1441-519.

ABSTRACT Electroencephalogram (EEG) signals reflect the activities or electrical disturbances in neurons in the human brain. Therefore, these signals are vital for diagnosing certain brain disorders. This study mainly focused on the diagnosis of epilepsy and autism spectrum disorders (ASDs) through the analysis and processing of EEGs. In this study, artifacts were removed from the EEG datasets using Independent Component Analysis and were filtered using a fifth-order band-pass Butterworth filter to remove interference and noise. Next, new methods were used to extract the features of EEGs using common spatial pattern (CSP). It is known that conventional CSP uses variance. However, here the use of entropy, energy, and band power with CSP was proposed to extract features of EEGs. Then, in our investigation, four techniques were employed for classification, namely, linear discriminant analysis, support vector machine, k-nearest neighbor (KNN), and artificial neural network, with the aim of comparing the proposed methods and recommending the optimal combination for the diagnosis of epilepsy and ASDs. Finally, the effects of segment length, frequency band, and reduction number on the results were investigated. Two EEG datasets were employed to verify the proposed methods: the King Abdulaziz University dataset (for ASD) and the MIT dataset (for epilepsy). The results indicated that the extracted features based on CSP and band LBP produced the best performance and that the combination of CSP-LBP-KNN provided the best performance with average classification accuracy of approximately 98.46% and 98.62% for diagnosing ASDs and epilepsy, respectively.

INDEX TERMS Artificial neural network, autism spectrum disorder, band power, brain–computer interface, common spatial pattern, electroencephalogram, energy, entropy, epilepsy, k-nearest neighbor, linear discriminant analysis, support vector machine.

I. INTRODUCTION

There are different techniques for reading brain activity: electroencephalography (EEG), magnetoencephalography (MEG), functional magnetic resonance imaging (fMRI), and functional near-infrared spectroscopy (fNIRS). Because neurons mutually communicate via electrical signals, which eventually reach the brain surface, EEG is used to capture brain activity through sensors (called electrodes) [1]. Lately, researchers in the multidisciplinary fields of engineering, neuroscience, microelectronics, bioengineering, and neurophysiology have made considerable efforts to utilize all of the information provided by EEG signals for many applications, such as an external device control, communications, and medical diagnosis. Currently, EEG-based signal-processing techniques are vital for diagnosing and monitoring neurological brain disorders because they help reflect the electrical activities or disorders of neurons in the human brain. Recently, brain disorders such as autism spectrum disorders (ASDs), epilepsy, and Alzheimer's have generally been considered the most important disorders focused on by researchers. Currently, diverse research is being conducted in this area to build and improve efficient diagnostic systems.

According to a reported study [2], globally, approximately 65 million people have epilepsy. Accordingly, many researchers have been developing computer systems to

The associate editor coordinating the review of this manuscript and approving it for publication was Mohammad Zia Ur Rahman.

diagnose this disease by analyzing the brain signals of affected individuals [3]. For example, Nigam and Graupe [4] suggested EEG-based computer-aided diagnosis to diagnose epilepsy using a multistage nonlinear pre-processing filter in combination with an artificial neural network (ANN); their proposed technique achieved accuracy of 97.2%. In addition, Kannathal *et al.* [5] compared different entropy algorithms and suggested that entropy values can distinguish between normal EEG and epileptic EEG; they used an adaptive neuro-fuzzy inference system (ANFIS) for classification and achieved accuracy of 92.2%. Moreover, Sadati *et al.* [6] used an adaptive neural fuzzy network instead of ANFIS for epilepsy diagnosis; they used the energy of discrete wavelet transform (DWT) sub-bands for feature extraction. However, their proposed method achieved low accuracy (about 85.9%). Ocak [7] also used approximated entropy for feature extraction, but in combination with DWT, and they achieved accuracy of over 96%; however, the accuracy was reduced to as low as 73% without DWT. Instead of only classifying sets A and E, Nunes *et al.* [8] considered the entire dataset (A, B, C, D, E) provided by Bonn University; they investigated several combinations of feature extraction and classification methods and achieved the best performance by using wavelet coefficients as feature extractors and the optimum-path forest classifier, which resulted in average accuracy of 89.2%. Subasi and Gursoy [9] studied different analyses to decrease the EEG data dimension, and they used the following techniques: principal component analysis (PCA), independent component analysis (ICA), and linear discriminant analysis (LDA). They also employed the wavelet transform technique for feature extraction and performed classification using an expert model; their proposed technique achieved accuracy of 94.5% [10]. Recently, a study [11] presented an fast Fourier transform (FFT) as a feature-extraction method and used the convolutional neural network (CNN) for classification; the proposed method achieved classification accuracy around 97.5%. Another recently developed method that also achieved classification accuracy of up to 98.78% was proposed by Li *et al.* [12] using wavelet-based envelope analysis for feature extraction and neural network ensemble as a classifier. Tzimourta *et al.* [13] presented a multicenter methodology for automated seizure detection based on DWT. The extracted feature vector was used to train a Random Forest classifier to achieve classification accuracy of 95%. In addition to all of the above, Zhang *et al.* [14] proposed a patient-independent diagnostic approach for epileptic seizure. The proposed approach refines the seizure-specific representation by eliminating the inter-subject noise through adversarial training.

Several studies aimed at designing a computer system for diagnosing ASDs have also been performed. For example, Sheikhani *et al.* [15] employed the short-time Fourier transform technique to extract features from EEG signals and then used the k-nearest neighbor (KNN) technique for classification. Their proposed method achieved overall accuracy of up to 82.4%. In addition, in their latest work [16], the team enhanced their approach and employed more data for testing (17 with ASDs and 11 normal subjects), obtaining classification accuracy of approximately 96.4%. Ahmadlou *et al.* [17] investigated the fractal dimension technique to measure the complexity and dynamic changes in the brains of patients suffering from ASDs; they achieved accuracy of 90% with a radial basis function classifier. Moreover, in another study [18], they diagnosed ASDs using the visibility graph method. Moreover, for the same task, they employed the fuzzy synchronization likelihood (Fuzzy SL) method and improved the probabilistic neural network (EPNN) classifier [19]. Both of the proposed methods [18], [19] achieved classification accuracy of approximately 95.5%. In [20], Bosl *et al.* conducted a study based on an EEG dataset that was collected from 79 subjects. They employed the minimum mean square error method to extract the features and used three types of classifier to differentiate normal signals from autistic ones: multiclass KNN, support vector machine (SVM), and naive Bayesian classification algorithms. The classification accuracy was over 80% at the age of 9 months. In particular, for boys, the classification accuracy was close to 100% at the age of 9 months, and it ranged from 70% to 90% at 12 and 18 months. For girls, the classification accuracy was highest at the age of 6 months, and it decreased for those older than that. The dataset in the work of Alhaddad *et al.* [21] was collected from 12 children: 8 boys with ASD and 4 without it. They employed optimum pre-processing techniques, time- and frequency-domain techniques [raw data and FFT] for feature extraction, and the Fisher linear discriminant technique for classification. Eventually, their proposed method achieved classification accuracy of up to 90%. In addition, Alsaggaf and Kamel [22] employed the same dataset and processing techniques that were employed in [21] to diagnose autism disorders; however, they did not use filtering techniques, so they achieved classification accuracy of 80.27%. Moreover, Fan *et al.* [23] conducted behavioral participation, enjoyment, frustration, boredom, and difficulty assessments to train a range of classification models, and employed the following classification techniques to compare the results: decision tree classifier, Bayes network, random forest, KNN, naive Bayes, SVM, and multilayer perceptron. Overall, their proposed methods achieved different classification accuracies that ranged from 75% to 85%. Recently, a study [24] presented automated identification of the severity of autism using empirical mode decomposition as a feature-extraction method and used the ANN for classification. The proposed method achieved overall classification accuracy of 97.2%. Another recent method that also achieved classification accuracy of 90.57% and 72.77% for SVM and KNN classifiers was proposed by Abdolzadegan *et al.* [25]. They used linear and nonlinear features such as power spectrum, wavelet transform, FFT, fractal dimension, correlation dimension, Lyapunov exponent, entropy, detrended fluctuation analysis, and synchronization likelihood for feature extraction. Elsewhere, Kang *et al.* [26] presented a study on the identification of autistic children. In that study, power spectrum analysis

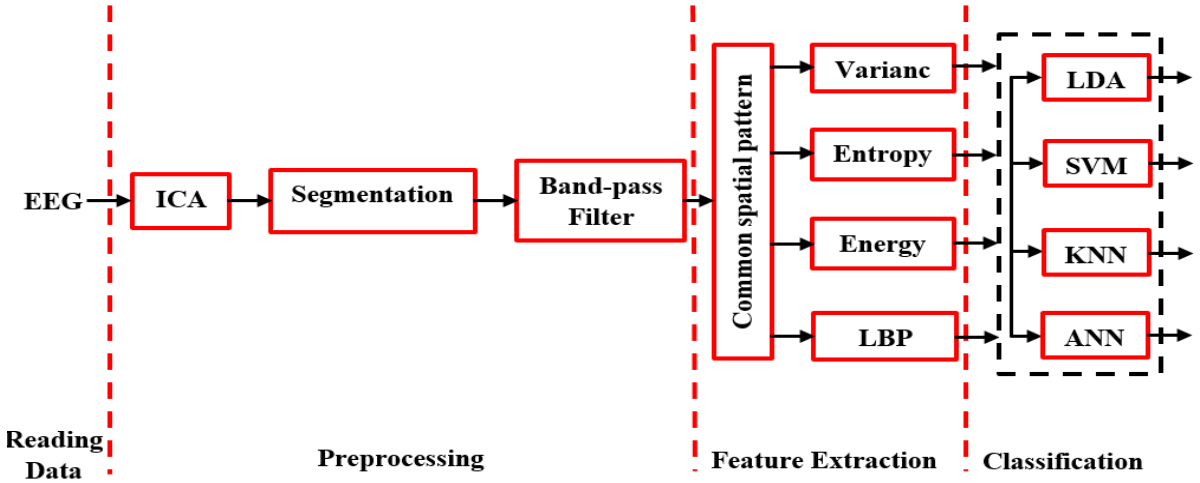

FIGURE 1. Block diagram of the proposed methods based on CSP.

was used for EEG analysis and areas of interest were selected for face gaze analysis of eye-tracking data. The SVM classifier was used to achieve the highest accuracy of 85.44%.

It is important to mention that feature extraction is one of the most important stages for improving classification accuracy. Most of the above-mentioned studies employed methods related to FFT or the wavelet transform to extract the features. However, to the best of our knowledge, no study has used the common spatial pattern (CSP) to extract the features of EEGs for diagnosing neurological diseases. Accordingly, in this study, we developed a new diagnostic system for diagnosing two neurological brain disorders: epilepsy and ASDs. A new feature-extraction method and several EEG-classification techniques are investigated to assist neurologists in accurately diagnosing those neurological brain disorders. After reading the EEG dataset, its artifacts and noise were removed and filtered in the pre-processing stage. First, the ICA technique was applied to remove the artifacts of EEG signals. Then, the EEG signals were segmented to fixed windows and fed to a band-pass Butterworth filter to remove the noise. Next, the CSP technique was used in order to extract the features of EEG signals. With CSP, we combined several techniques, such as energy, entropy, and band power (BP), in order to improve the average classification accuracy. In addition, for further investigation, we used four types of classifier: LDA, SVM, KNN, and ANNs. We also investigated the effects of segment length, frequency band, and reduction number on the classification accuracy.

The remainder of this paper is organized as follows. Section 2 describes the used EEG data and the following EEG signal-processing methods: pre-processing, feature extraction, and classification techniques. The results and the discussion are presented in Section 3. Finally, the conclusion and some future work prospects are presented in Section 4.

II. METHODS

In this section, the proposed methods for processing the EEG signals, including the data description, pre-processing, feature extraction, and classification techniques, are described. These methods are also verified using MATLAB simulation tools in the next section. Figure 1 shows a block diagram of the proposed methods. First, the EEG data were read and then the ICA technique was used to remove artifacts from the raw EEG dataset. Next, the EEG signals were segmented into fixed time windows. Subsequently, the output of the segmentation procedure was introduced into the band-pass filter. After that, the output of the filtering process was fed into the CSP algorithm (i.e., CSP was applied to the filtered signals). Afterward, the feature vectors were extracted by introducing the CSP output into the variance, entropy, energy, and logarithmic BP (LBP). The LDA, SVMs, KNN algorithm, and ANN techniques were then employed as classifiers. Finally, all of the possible combinations of the proposed approaches were implemented and verified. In the following subsections, each stage is discussed in more detail, from the data description to the classification process.

A. DATASET DESCRIPTION

Because two types of disorder were investigated (epilepsy and autism), two types of dataset were employed to verify our methods: the first for autism and the second for epilepsy. We obtained the autism dataset from the Brain and Computer Interface Group at King Abdulaziz University, Jeddah, Saudi Arabia; this dataset was recorded using subjects in a relaxed state and divided into two groups. The first group is called the natural (normal) group and contains 10 healthy volunteers (all males, aged 9–16) with normal intelligence and without any mental disorders. The second group is called the autism group and contains nine patients (six males and three females, ages 10–16 years) with ASDs. EEG signals were recorded from the scalps of these subjects while they were in a relaxed state by using an EEG data-acquisition system comprising the following components: a g.tec EEG cap with 16 high-accuracy Ag/AgCl electrodes (Fp1, Fp2, Fz, F3, F4, F7, F8, Cz, C3, C4, T3, T5, Pz, Oz, O1, and O2) based on 10–20 international acquisition systems, g.tec USB

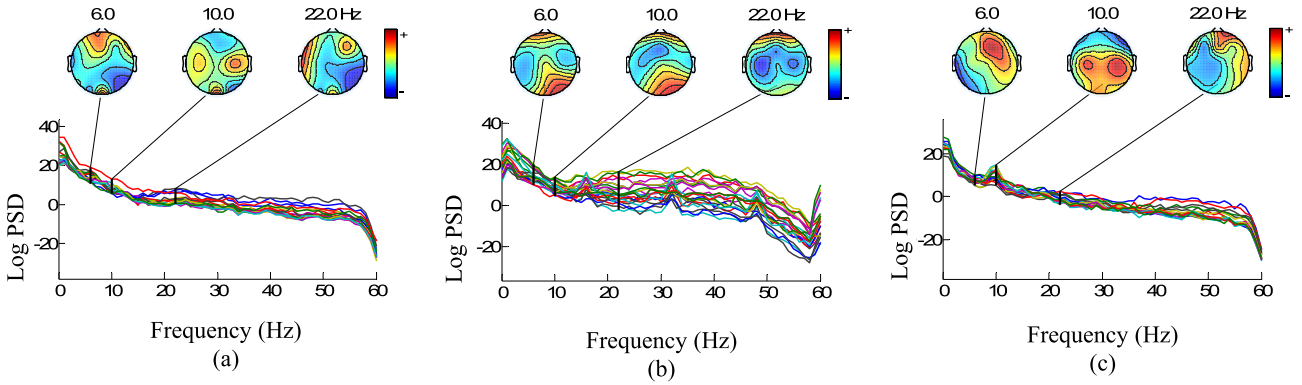

FIGURE 2. Power spectral density and electrode map for (a) autistic EEG, (b) epileptic EEG and (c) normal EEG [29].

amplifiers, and BCI2000 software. The dataset was filtered using a band-pass filter (frequency band: 0.1–60 Hz) and a notch filter (stop-band frequency: 60 Hz). All of the EEG signals were digitized when the sampling frequency was 256 Hz. For the healthy volunteers, the EEG recordings varied from 5 to 27 min with total time of 148 min. However, for the autistic patients, the recordings varied from 12 to 40 min with a total of 173 min.

The second dataset is the CHB-MIT dataset, which was collected at the Children's Hospital in Boston. This dataset consists of EEG recordings of pediatric subjects with severe seizures. EEG signals were recorded from 22 people: 17 females and 5 males. The females' ages ranged from 1.5 to 19 years, while those of the males ranged from 3 to 22 years. There are 686 recordings grouped into 23 cases. The duration of each recording is 1, 2, or 4 h. Recordings belonging to case 10 are 2 h long, recordings belonging to cases 4, 6, 7, and 9 are 4 h long, while the rest are 1 h (the total number of recording hours is 906). Records with at least one seizure are classified as seizure records and those without seizures are classified as non-seizure ones. The total number of seizures in these recordings is 198. All signals were sampled at 256 samples per second with 16-bit resolution. The International 10–20 system of EEG electrode positions and nomenclature were used for these recordings. For more details on these data, please refer to these references [27], [29].

Figure 2 shows EEG power spectral density (with a logarithmic scale) and electrode maps for autistic, epileptic, and normal subjects. The electrode map is shown for three different arbitrary frequencies: 6, 10, and 22 Hz. In general, the low-frequency spectrum has higher power density than the high-frequency one. Comparing the three subjects, we see different power spectral density patterns.

B. PRE-PROCESSING

During the EEG dataset recording, the artifacts, noise, and interference were recorded as well. These were generated from the electrodes, the magnetic fields of the electronic devices, blood pressure, breathing, limb movements, eye blinking, or other human movements [30]. In the pre-processing stage, the ICA technique was used to remove the eye blinking artifacts. Four channels around the eyes were used as references to remove the eye blinking artifacts. Then, the EEG data were divided into M segments, each having a size of $(ch \times T)$, where ch denotes the number of channels and T (time windows) denotes the number of EEG samples per channel in a specific time interval T. In this study, different time windows were applied for investigation. After the windowing signals, the segmented signals were filtered using a fifth-order band-pass Butterworth filter to remove the interference and noise generated owing to the electrodes and the magnetic fields of the other devices. In this study, different frequency bands were used for investigation.

C. FEATURE EXTRACTION

Several feature-extraction techniques are available. Here we used a popular technique, namely, CSP. Originally, CSP was based on variance. However, we propose the use of CSP based on entropy, energy, and LBP.

1) COMMON SPATIAL PATTERN

We used the CSP algorithm as a spatial filter that leads to peak variances for differentiating between the two classes of EEGs (normal and epilepsy/autism) [31]. The computed projection matrix comprises a set of CSP filters. The algorithm starts by computing the normalized spatial covariance for both classes, which is achieved using the following equations:

$$C_{CI} = \frac{E_{CI}E_{CI}'}{trace(E_{CI}E_{CI}')} \qquad C_{CII} = \frac{E_{CII}E_{CII}'}{trace(E_{CII}E_{CII}')} \quad (1)$$

where E_{CI} and E_{CII} denote the two single segments under two conditions (class I and class II) of size $ch \times T$, where ch is the number of channels and T is the number of samples per channel. E' is the transpose of E, and $trace(EE')$ is the sum of the diagonal elements of EE'. Then, the averaged normalized covariances $\overline{C_{CI}}$ and $\overline{C_{CII}}$ are calculated by averaging all of the segments of each class. The overall composite spatial covariance is given by:

$$C_C = \overline{C_{CI}} + \overline{C_{CII}} \quad (2)$$

and factorized into eigenvalues and eigenvectors, such as

$$C_C = U_C \lambda_C U_C' \tag{3}$$

where U_C is the matrix of the eigenvectors and λ_C is the diagonal matrix of the eigenvalues. All of the eigenvalues are arranged in descending order. Subsequently, the whitening transformation P is computed as follows:

$$p = \sqrt{\lambda_C^{-1}} U'_C \tag{4}$$

Then, we have to find

$$S_{CI} = P\overline{C_{CI}}P' \text{ and } S_{CII} = P\overline{C_{CII}}P' \tag{5}$$

To test these calculations, the sum of the corresponding eigenvalues of SCI and SCII should be an identity matrix, and SCI and SCII should have the same eigenvectors:

$$S_{CI} = B\lambda_{CI}B' \tag{6}$$

$$S_{CII} = B\lambda_{CII}B' \tag{7}$$

$$\lambda_{CI} + \lambda_{CII} = I \tag{8}$$

where B is any orthonormal matrix that satisfies

$$B'(S_{CI} + S_{CII})B = I. \tag{9}$$

The largest eigenvalues with the corresponding eigenvectors for S_{CI} have the smallest eigenvalues for S_{CII}, and vice versa. This demonstrates the maximization of the eigenvalues of one class at a point and the minimization of the eigenvalues of the other class at the same point. Thus, the covariance between the two classes is successfully maximized. A set of CSP filters (projection matrix) can be obtained as

$$W_{Csp} = P'B = [w_1 w_2 \ldots w_{ch-1} w_{ch}] \in R^{ch \times ch} \tag{10}$$

The first CSP filter w_1 provides the maximum variance of class I, and the last CSP filter w_{ch} provides the maximum variance of class II. For dimensionality reduction, only the first and last m filters may be used, such that

$$W_{Csp} = [w_1 w_2 \ldots w_m w_{ch-m+1} w_{ch-m} \ldots w_{ch}] \in R^{2m \times ch}, \tag{11}$$

and the filtered signal $S(t)$ is given by

$$s(t) = W_{Csp} e(t) = [s_1(t)\, s_2(t) \ldots s_d(t)]' \tag{12}$$

where d is the reduction number, which is equal to $2 \times m$. The reduction number is the number by which the channels should be reduced. Thus, for each class's EEG sample matrix, we may select the small number of signals (m) that are most important for the differentiation between the two classes. Finally, the feature vectors $f = (f_1, f_2, f_3, \ldots, f_{2m})'$ can be calculated using the following equation:

$$f_i(var) = \log\left[\frac{var[s_i(t)]}{\sum_{i=1}^{2m} var[s_i(t)]}\right] \tag{13}$$

Thus, the d features were obtained for each segment as a result of the common spatial filtering. In addition to the logarithmic variance, in this study, we propose extracting the features using energy, entropy, and LBP, which are defined as follows:

Entropy Features:

$$f_i(Entropy) = \sum_{n=1}^{N} |s_i(t)|^2 \log |s_i(t)|^2 \tag{14}$$

Energy Features:

$$f_i(Energy) = \sum_{n=1}^{N} |s_i(t)|^2 \tag{15}$$

LBP Features:

$$f_i(LBP) = \log\left[\frac{1}{N}\sum_{n=1}^{N} |s_i(t)|^2\right] \tag{16}$$

As a result, by means of CSP, each segment will be transformed into a feature vector of length d. Thus, the size of the feature matrix resulting from the CSP is $M \times d$, where M is the number of segments and d is the reduction number as mentioned above. In this study, we investigated the effects of M and d on the classification accuracy of both autism and epilepsy disorders (Tables IV, V, VIII, and IX). The formed feature matrix was fed into the classification and cross-validation stage as discussed in the following subsection.

D. CLASSIFICATION AND CROSS-VALIDATION

Several classification algorithms are available. However, in this study, we employed the most widely used classification techniques to classify the obtained features: LDA, SVM, KNN, and ANN. Our main aim was to compare them and determine which one best classifies normal, epilepsy, and autism cases.

The LDA and SVM classification techniques use hyperplane separation to classify their entries. LDA is Fischer's linear discrimination, which relies on the mean vectors and the covariance matrices of the feature vectors of the individual categories (classes). LDA also uses a hyperplane method to distinguish different categories, reduce the variances within categories, and exploit the variances between categories [32]. SVM is a supervised learning method that analyzes data and identifies patterns; it is used for classification and regression analysis. Considering a set of training examples, the SVM training algorithm builds a model (e.g., hyper-level separation) that assigns new examples into individual classes [33]. KNN is one of the simplest machine-learning algorithms, which classifies an entity according to the majority vote of its k-nearest neighbors [34]. In this study, k was selected as 3 for all experiments. We also employed the ANN technique for classification, as it is an information-processing technique that simulates the processes of human cognition. In the training process, feature vectors were fed to the ANNs to adjust their variable parameters, weights, and biases. Thus, the relationship between the input and output patterns was defined. In this study, we developed an ANN system with a single input layer, a single hidden layer, and a single output layer using MATLAB. The hidden and output layers were designed with five and two nodes, respectively. However,

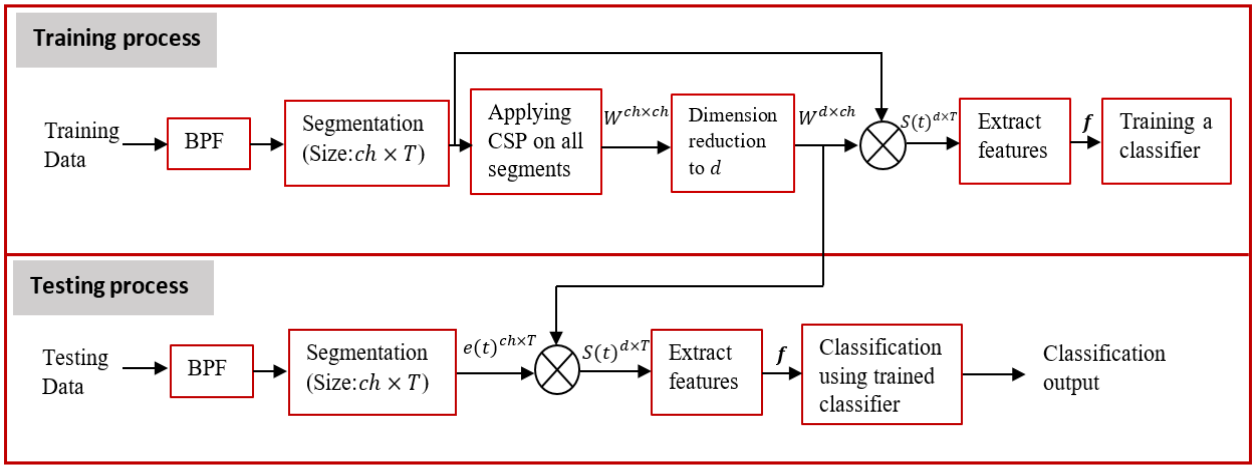

FIGURE 3. Applying CSP in training and testing phases.

the number of nodes was based on the number of features obtained from the vectors. In addition, we changed the hidden and output layers' transfer functions to "logsig" and "softmax," respectively, the train function to "trainbr," learning training to 0.01, and other parameters as well. All of these adjustments were made to obtain better results.

Moreover, we used the k-fold cross-validation technique to obtain the classification accuracy. In this technique, the dataset is arbitrarily separated into k equal parts (k subsets) [35], where one subset is used for validation (test) and the other subsets are used for training. The cross-validation is repeated k times (fold). Then, the results of the k times are averaged to obtain a single classification rate. In this study, we employed 5-fold cross-validation, which means 20% for testing and 80% for training. The classification accuracy is given by

$$accuracy = \left(\frac{N_{correct}}{N_{total}}\right) \times 100\% \tag{17}$$

where N_{total} is the overall number of vectors to be classified and $N_{correct}$ is the number of correct vectors.

The performance of a classification model can also be evaluated by plotting the receiver operating characteristic (ROC) curve. This curve plots two parameters, true positive rate and false positive rate, which are defined as:

$$TPR = \frac{\text{TP}}{\text{TP} + \text{FN}} = sensitivity \tag{18}$$

$$FPR = \frac{\text{FP}}{\text{FP} + \text{TN}} = 1 - specificity \tag{19}$$

where TP is true positive, FN is false negative, FP is false positive, and TN is true negative. The area under the ROC curve (AUC) is a common metric that can be used to compare different tests. AUC ranges in value from 0 to 1; if AUC is close to 1 (area of unit square), this indicates a very good test. A reference [36] contains more details about ROC-AUC curves.

Figure 3 shows the application of CSP in the training and testing phases. Initially, as mentioned above, the data are divided into two parts: 80% of the data for training and 20% for testing. Diagnosis of a disorder using signal processing begins with the training phase, followed by the testing phase. The training phase begins with filtering the training data using BPF. Then, the filtered signals are divided into M equal segments: the size of each segment is $ch \times T$. The number of segments depends on the length of one segment: the larger the segment length, the smaller the number M, and vice versa. After segmenting the signals, CSP is applied to all of the segments (both normal and epileptic/autistic) that we obtained according to Eq. (1) through Eq. (10) to obtain the projection matrix $W^{ch\times ch}$, a set of CSP filters. After this, the dimensions of this matrix are reduced by selecting the first and last m filters for obtaining the matrix $W^{d\times ch}$, as described in Eq. (11). Each segment is then filtered (multiplied) by $W^{d\times ch}$, according to Eq. (12). (The size of each filtered segment is dxT.) The last but one process is the formation of one feature vector f from one filtered segment: that is, the number of feature vectors will be equal to the number of segments M that we obtained from the segmentation process. The element number of one feature vector is d: $f = (f_1, f_2, f_3, \ldots, f_d)'$. The elements of the vector are calculated using variance, entropy, energy, or BP according to equations (13)–(16), respectively. The last process in the training phase is the training of a classifier (LDA, SVM, ANN, or KNN) using the feature vectors obtained from the previous step, so that the classifier is told that these feature vectors belong to healthy people while the other vectors belong to epileptic/autistic people. There processes are similar between the training and testing phases. The testing data are filtered using BPF and segmented in a similar way as in the training phase. The difference is that the CSP is not applied to the segments, but they are directly filtered using the $W^{d\times ch}$ matrix that was produced in the training phase. Then, the feature vectors are formed in a manner similar to

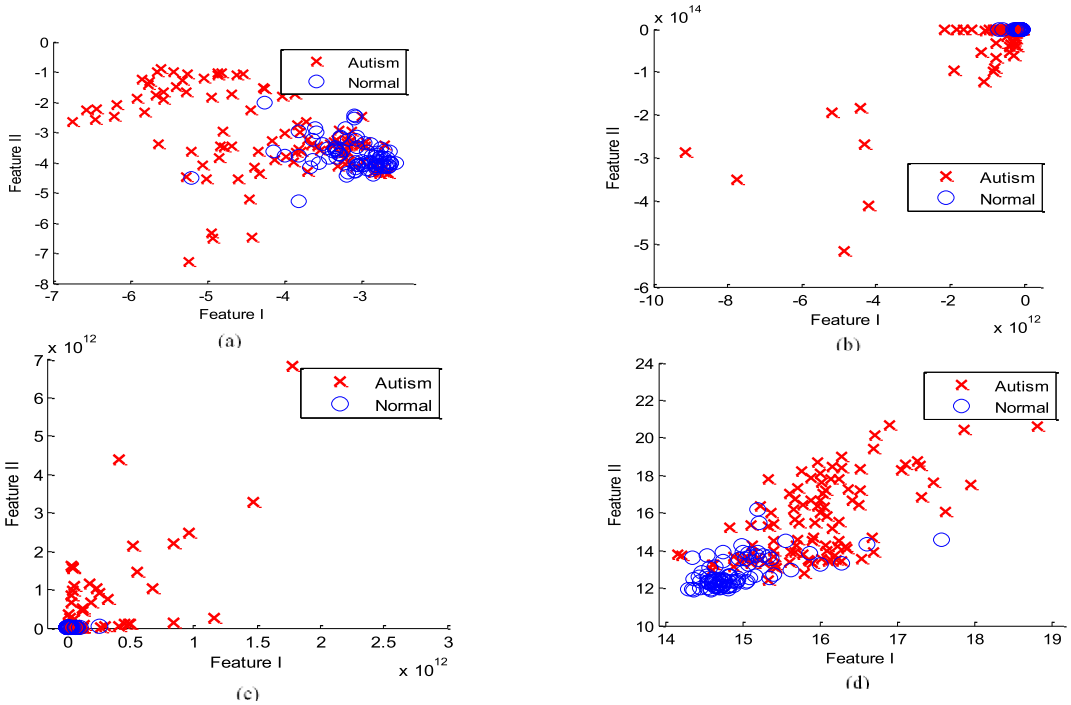

FIGURE 4. 2D plot the feature vectors of the autsim and normal data using (a) CSP+variance, (b) CSP+entropy, (c) CSP+energy, and (d) CSP+LBP.

that explained in the training phase. The last process in the testing phase is introducing feature vectors to the classifier, which has been trained in the training phase, to classify the feature vectors: which of them belong to healthy people and which to epileptic/autistic ones. The classification accuracy is then calculated according to Eqs. 17–19, taking into account the application of the cross-validation technique described in the previous paragraph.

III. RESULTS AND DISCUSSION

As mentioned above, we used two types of data: autistic and epileptic data. Before the feature-extraction process, the signals were first segmented to a time window of 50 s and then filtered by a band-pass Butterworth filter having a frequency band of 0.5–60 Hz. Next, the features were extracted using the CSP algorithm in combination with the following statistical methods: variance, entropy, energy, and BP. Figures 4 and 5 show a 2D plot of the feature vectors extracted by all of the approaches. The plots of the extracted features from the autistic dataset are shown in Fig. 4, while Fig. 5 shows the plots of the features extracted from the epileptic dataset. As shown in Fig. 4(a) and 5(a), the CSP-variance method did not provide peak variances as expected in [37] for discriminating the normal versus epileptic/autistic features. This made the features proximal to each other. To separate these features and redistribute them, we proposed extracting new features using entropy, energy, and LBP. It is clear from Fig. 4 and 5 that the features extracted by the CSP-LBP method can be better separated than those extracted using other approaches.

Band power is a commonly used method in EEG analysis for estimating the power of EEG signals [38]. In this study, we perform conventional CSP but replace variance with BP. The variance is defined by $\frac{1}{N}\sum_{n=1}^{N}(s_i(t)-\mu_i)^2$, which is similar to (16) if the mean value is ignored. We also retain the use of logarithmic operation as normally used in the CSP-variance method. This modification redistributes the normal and epileptic/autistic features for easy classification [39]. As shown in Fig. 4, autistic EEG has energy and LBP values that are higher than normal, while the variance and entropy values are lower than normal. The same findings can be observed in the case of epileptic EEG, as in Figure 5. As mentioned previously, the BP estimates the average power of EEG signals.

TABLE 1. Classification accuracy using KNN (normal vs. autistic).

Feature Extraction	Classification accuracy	
	Mean (%)	SD
CSP + Variance	93.88	2
CSP + Entropy	94.93	1.4
CSP + Energy	**95.42**	**2.2**
CSP + LBP	**95.48**	**2.1**

After extracting the features, the KNN technique was used to classify the features extracted by the CSP + variance, CSP + entropy, CSP + energy, and CSP + BP methods. Tables I–III present classification accuracies in terms of mean and standard deviation (SD). Table 1 gives a comparison of

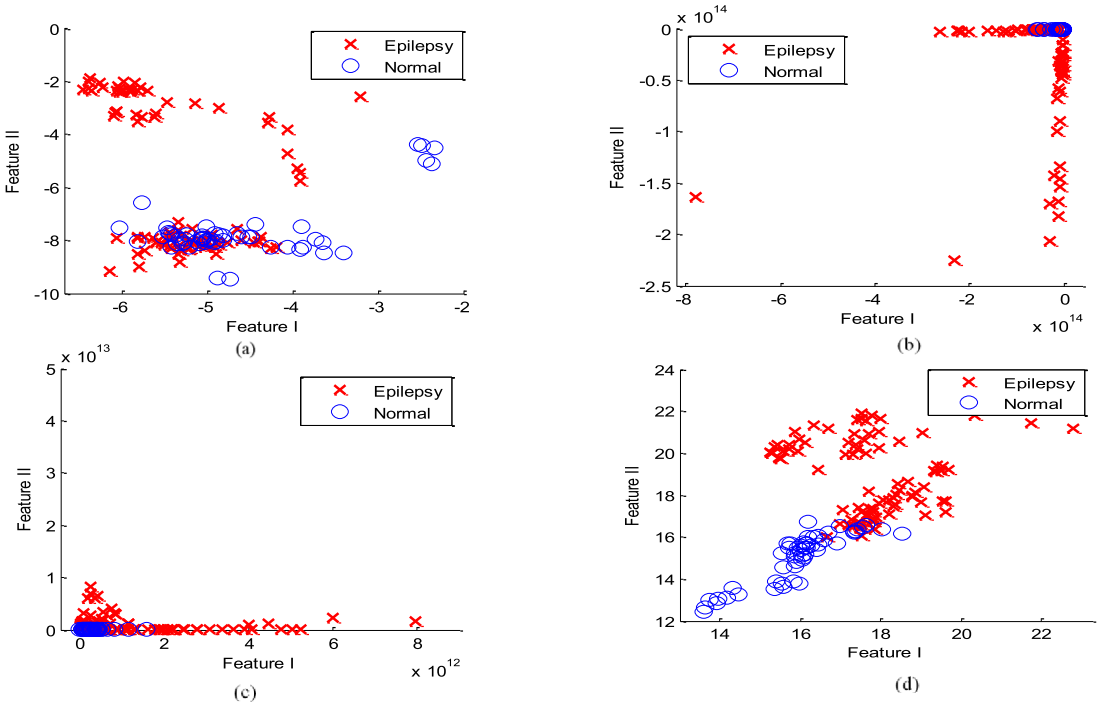

FIGURE 5. 2D plot the feature vectors of the epilepsy and normal data using (a) CSP+variance, (b)CSP+entropy, (c) CSP+energy, and (a) CSP+LBP.

TABLE 2. Classification accuracy using KNN for normal vs. epilepsy.

Feature Extraction	Classification accuracy	
	Mean (%)	SD
CSP + Variance	93.14	3.10
CSP + Entropy	96.60	3.60
CSP + Energy	**97.70**	**4.10**
CSP + LBP	**97.20**	**0.03**

TABLE 3. Classification accuracy using KNN (autistic vs. epilepsy).

Feature Extraction	Classification accuracy	
	Mean (%)	SD
CSP + Variance	**99.96**	**0.610**
CSP + Entropy	97.83	0.010
CSP + Energy	97.82	1.500
CSP + LBP	**99.50**	**0.015**

the classification accuracies of the features extracted from the normal data and those from the autistic data. It can be seen that the features extracted by CSP + energy and CSP + LBP provided better results with average classification accuracies of 95.42% and 95.48% with SDs of 2.2 and 2.1, respectively. Table 2 gives a comparison of the classification accuracies of the features extracted from the normal data and those from the epileptic data. As seen in Table 2, the features extracted by CSP + energy and CSP + LBP have the highest average classification accuracies of 97.70% and 97.20% with SD of 4.10 and 0.03, respectively. For further investigation of the proposed approaches, we performed classification of the autistic features versus the epileptic features. The results are shown in Table 3, which indicates that the best results were obtained from the CSP + variance and CSP+LBP methods with average classification accuracy of 99.96% and 99.50%. We note from these three tables that the features resulting from the CSP+LBP method have the highest classification accuracy and the smallest SD. A smaller standard deviation means that the classification accuracies produced by 5-cross validation do not deviate much from the mean, which makes the CSP+LBP method more stable than the other methods.

For further investigation, three additional techniques were used for classification. Specifically, in addition to the KNN technique, the LDA, SVM, and ANN techniques were also employed. Figure 6 shows a comparison of these classification methods, which classify the normal versus autistic features extracted using all of the proposed approaches. From this figure, two important observations can be made: first, the KNN classifier provides the highest classification accuracy with all of the proposed feature-extraction approaches. Second, the CSP+LBP method provides the best results regardless of the type of classifier used. However, the CSP+LBP method works better with the KNN classifier. Figures 7 and 8 also show a comparison of the classification

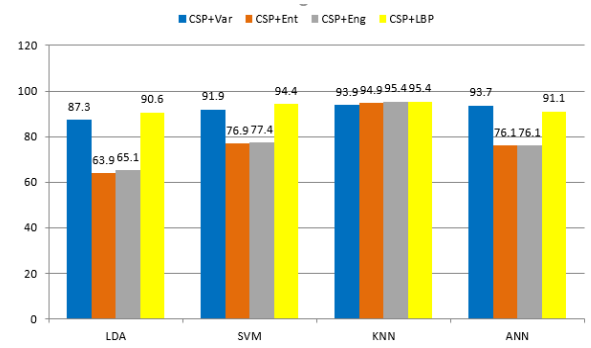

FIGURE 6. Average classification accuracy (normal vs. autistic) using LDA, SVM, KNN, and ANN.

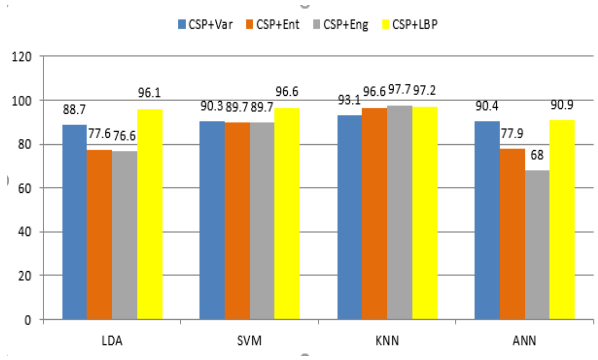

FIGURE 7. Average classification accuracy (normal vs. epileptic) using LDA, SVM, KNN, and ANN.

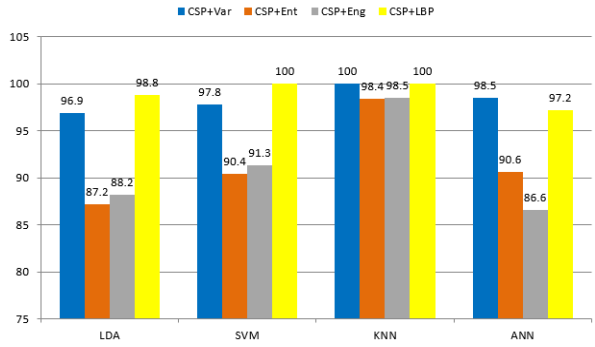

FIGURE 8. Average classification accuracy (autistic vs. epilepsy) using LDA, SVM, KNN, and ANN.

methods for the normal versus autistic features and autistic versus epileptic features, respectively. The same two previous observations can be confirmed in these figures.

For further verification of classifier performance, Figures 9–11 show ROC curves along with AUC for the four classifiers: LDA, SVM, KNN, and ANN. Figure 9 shows ROC-AUC related to the classification of autism CSP-LBP features versus normal CSP-LBP features. We note that the performance of the KNN classifier is the best, as the area under the curve (the blue color) is larger than the other areas. From the figure, we also note that SVM and LDA classifiers provide good performance. Figure 10 shows ROC-AUC for epileptic/normal CSP-LBP, while Figure 11 shows ROC-AUC for autistic/epileptic CSP-LBP. The same findings

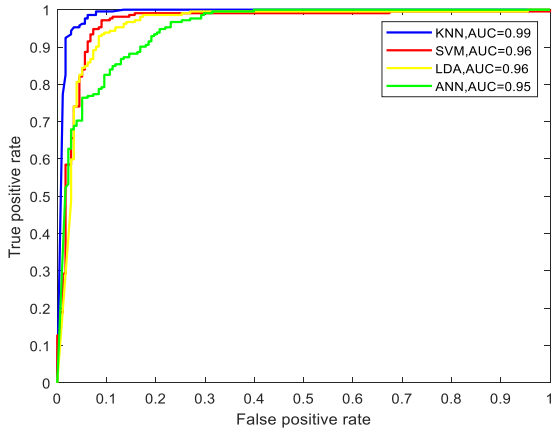

FIGURE 9. ROC-AUC based on CSP+LBP features (autism vs. epilepsy).

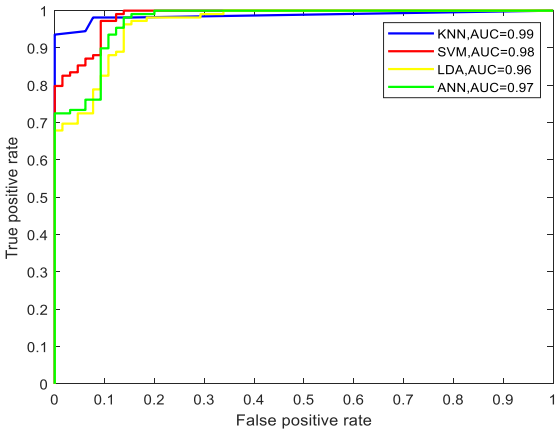

FIGURE 10. ROC-AUC based on CSP+LBP features (epileptic vs. normal).

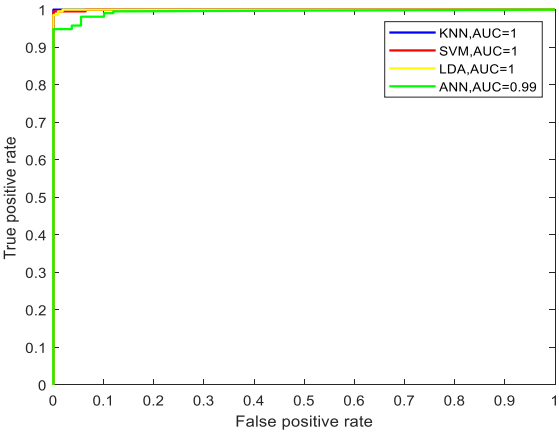

FIGURE 11. ROC-AUC based on CSP+LBP features (autistic vs. epileptic).

from Figure 9 can also be found in Figures 10 and 11, in that KNN performs the best, followed by SVM, then LDA, and finally ANN.

A. EFFECT OF SEGMENT LENGTH

Thus far, all of the signals, from either the autistic or the epileptic dataset, were segmented into time windows of 50 s, as mentioned above. Now, we investigate the effect

TABLE 4. Effect of segment length on classification accuracy (normal vs. autistic).

0.5–60Hz Segment length (s)	Method				
	No. of segments (M)	CSP + LBP + LDA	CSP + LBP + SVM	CSP + LBP + KNN	CSP + LBP + ANN
10	1971	87.87	96.05	96.60	90.46
20	985	87.00	95.63	96.35	91.55
30	656	86.42	94.50	96.34	90.82
40	492	89.03	94.65	95.49	89.58
50	**393**	**96.05**	**96.63**	**97.17**	**90.92**
60	328	89.02	93.20	96.34	92.63
70	281	90.77	92.86	95.39	90.03
80	246	88.98	93.12	95.52	86.53
90	218	88.59	93.14	93.57	87.21
100	196	91.84	92.37	93.39	89.76

TABLE 5. Effect of segment length on classification accuracy (normal vs. epileptic).

0.5-60Hz Segment length (s)	Method				
	No. of segments (M)	CSP + LBP + LDA	CSP + LBP + SVM	CSP + LBP + KNN	CSP + LBP + ANN
10	876	93.95	96.57	97.72	87.56
20	438	94.07	97.27	97.49	83.41
30	**292**	**95.87**	**97.26**	**97.95**	**92.85**
40	218	97.25	95.93	97.25	89.45
50	175	94.35	95.52	97.09	89.12
60	146	94.61	95.86	96.57	91.71
70	125	96.03	98.40	99.23	79.29
80	109	98.18	98.18	99.09	83.27
90	96	94.56	96.78	96.89	82.33
100	87	97.89	98.89	98.89	84.72

TABLE 6. Effect of frequency band on classification accuracy (normal vs. autistic).

Segment length: 50 s Frequency band	Method			
	CSP + LBP + LDA	CSP + LBP + SVM	CSP + LBP + KNN	CSP + LBP + ANN
Delta (1–4Hz)	91.85	92.87	95.69	91.10
Theta (4–8Hz)	93.38	**96.94**	97.96	91.37
Alpha (8–15Hz)	93.38	96.44	96.94	94.92
Beta (15–30Hz)	90.08	94.65	97.96	88.85
Gamma (30–60Hz)	84.44	92.58	96.42	90.59
1–30 Hz	92.88	95.17	97.46	93.15
4–30 Hz	**92.13**	**95.40**	**98.21**	**95.69**
8–30 Hz	89.82	94.91	97.19	94.16
1–40 Hz	**93.88**	94.91	96.68	91.34
8–40 Hz	90.83	94.65	97.21	93.16
4–60 Hz	91.58	93.38	96.95	84.41
8–60 Hz	90.10	94.93	95.95	92.91

of the segment length on the results. Because the highest classification accuracy was obtained by the CSP + LBP feature-extraction method, CSP + LBP was used in this investigation. Table 4 gives the effect of the segment length in the autistic dataset. The first two columns in Table 4 list the segment length and the corresponding number of segments,

TABLE 7. Effect of frequency band on classification accuracy (normal vs. epileptic).

Segment length: 30 s **Frequency band**	**Method**			
	CSP + LBP + LDA	**CSP + LBP + SVM**	**CSP + LBP + KNN**	**CSP + LBP + ANN**
Delta (1–4Hz)	94.84	95.21	97.59	88.69
Theta (4–8Hz)	93.82	94.51	97.60	92.80
Alpha (8–15Hz)	91.41	92.78	94.51	89.69
Beta (15–30Hz)	84.57	89.09	90.49	85.28
Gamma (30–60Hz)	88.07	89.74	91.45	86.64
1–30 Hz	94.86	96.23	97.25	81.47
4–30 Hz	94.16	93.51	96.57	**93.44**
8–30 Hz	89.40	90.03	92.80	83.31
1–40 Hz	**95.89**	**96.90**	**97.93**	**88.62**
8–40 Hz	87.99	91.44	94.86	85.92
4–60 Hz	94.18	94.49	95.22	86.31
8–60 Hz	86.94	93.46	92.45	86.60

TABLE 8. Effect of reduction number on classification accuracy (normal vs. autistic).

Segment length: 50 s 4–30 Hz reduction number (d)	**Method**			
	CSP + LBP + LDA	**CSP + LBP + SVM**	**CSP + LBP + KNN**	**CSP + LBP + ANN**
2	77.10	84.23	90.10	84.19
4	78.60	90.81	95.43	84.21
6	76.88	93.37	95.91	87.81
8	80.67	92.35	95.92	89.59
10	82.69	93.92	96.45	89.29
12	85.72	93.63	96.96	91.10
14	89.79	93.87	98.21	92.62
16	**93.40**	**95.92**	**98.46**	**94.15**

and the other four columns list the classification accuracies according to the LDA, SVM, KNN, and ANN techniques. It can be observed from Table 4 that, as the window length increases from 10 to 100, the number of segments decreases; moreover, the classification accuracy begins to increase to a certain value and then starts to decrease. Thus, it is important to choose the optimal length and a suitable number of segments, which give the highest classification accuracy. In this case, the optimal segment length is 50 s and the corresponding number of segments is 393. Table 5 depicts the effect of the segment length in the epileptic dataset. The results here are slightly different. It can be seen that, as the segment length increases from 10 to 100, the classification accuracy starts to increase to a certain value, then begins to decrease, and then starts increasing again. The highest value of accuracy reached was 98.89%, but the number of segments decreased to 50. Thus, in this case, the optimal segment length was 30 s and the corresponding number of segments was 292, which is acceptable. At a segment length of 30 s, the highest classification accuracy of 97.95% was obtained by a combination of CSP + LBP + KNN.

B. EFFECT OF THE FREQUENCY BAND

In general, the frequency range of EEG signals extends from 0 to 100 Hz, which is divided into sub-bands: delta (<4 Hz), theta (4–8 Hz), ýalpha (8–13 Hz), beta (13–30 Hz), and gamma (>30 Hz). Raw EEG signals may contain noise from different sources, such as electric or electromagnetic fields. In autistic and epileptic signals, important data may not be concentrated in constant-frequency bands. Therefore, before feature extraction, the use of a frequency filter is vital for removing the unwanted frequency components and passing the desired components. Accordingly, all of the results were obtained after filtering the EEG signals using

TABLE 9. Effect of reduction number on classification accuracy (normal vs. epileptic).

Segment length: 30 s 1–40 Hz reduction number (d)	Method			
	CSP + LBP + LDA	CSP + LBP + SVM	CSP + LBP + KNN	CSP + LBP + ANN
2	85.30	90.78	91.76	91.78
4	90.38	93.83	96.92	93.83
6	92.16	96.26	96.94	89.79
8	93.16	96.25	97.62	94.20
10	91.41	96.55	97.59	90.40
12	93.84	96.57	97.60	92.45
14	91.85	96.59	97.61	91.44
16	**94.17**	**96.92**	**98.62**	**93.48**
18	93.47	97.24	97.59	92.11
20	95.22	96.94	97.29	90.76
22	94.87	97.26	97.62	89.41

TABLE 10. Summary of best methods for autism and epilepsy diagnosis.

	Methods							
	CSP + LBP + LDA		CSP + LBP + SVM		CSP + LBP +KNN		CSP + LBP + ANN	
	Mean%	SD	Mean%	SD	Mean%	SD	Mean%	SD
Normal vs. autism Segment length: 50 sec BPF: 4–30 Hz Reduction number: d=16	93.40	4	95.92	2.5	**98.46**	0.042	94.15	5.76
Normal vs. epileptic Segment length: 30 sec BPF: 1–40 Hz Reduction number: d=16	94.17	6.2	96.92	0.14	**98.62**	3.15	93.48	8.3

TABLE 11. Comparison of the classification results for ASD diagnosis.

The authors	Feature Extraction	Classification	Dataset	Accuracy
Sheikhani et al. [15]	STFT	KNN	Own dataset	82.4
Sheikhani et al. [16]	STFT and statistical	KNN	Own dataset	96.4
Ahmadlou et al. [17]	Wavelet and fractal dimension	RBNN	Iranian dataset	90
Ahmadlou et al. [18]	Wavelet and visibility graph	EPNN	Iranian dataset	95.5
Ahmadlou et al. [19]	Wavelet and fuzzy logic	EPNN	Iranian dataset	95.5
Bols et al. [20]	Modified multiscale	SVM	Own dataset	70–100
Alhaddad e al [21]	FFT	FLDA	Own dataset	90
Alsaggaf et al. [22]	FFT	FLDA	Own dataset	80.27
Hadoush et al. [24]	EMD	ANN	Jordan University of Science and Technology	94.4
Abdolzadegan et al. [25]	Wavelet+FFT	SVM,KNN	Own dataset	90.57
Kang et al. [26]	AOI & MRMR	SVM	Own dataset	85.44
Our work	**CSP-LBP**	**KNN**	King Abdulaziz university	**98.46**

a 60-Hz band-pass filter. Here, we used a segment length of 50 s to investigate the effect of the filter's frequency band on the results. Table 6 gives the classification accuracies of the autistic data versus the normal data at different

TABLE 12. Comparison of the classification results for epilepsy diagnosis.

The authors	Feature Extraction	Classification	Dataset	Accuracy%
Nigam et al. [4]	Non-linear filter	ANN	Bonn university	97.2
Kannathal et al. [5]	Entropies	ANFIS	Bonn university	92.2
Sadati et al. [6]	DWT	SNFN	Bonn university	86
Ocak [7]	Apen +DWT	ANN	Bonn university	96
Nunes et al. [8]	wavelet	Optimum path forest	Bonn university	89.2
Subasi [9]	DWT	Mixture of expert model	Bonn university	94.5
Zhou et al. [11]	FFT	CNN	CHB-MIT	97.5
Li et al.[12]	wavelet	NNE	Bonn university	98.78
Tzimourta et al. [13]	DWT	Random Forest	Bonn university	95
Khan et al. [39]	DWT	LDA	CHB-MIT	91.8
Our work	**CSP-LBP**	**KNN**	CHB-MIT	**98.62**

frequency bands. It can be seen from Table 6 that changing the frequency band leads to a change in the classification accuracy. According to the results presented in Table 6, the highest accuracy was obtained when the EEG signals were filtered using a 4–30-Hz band-pass filter. Table 7 gives the classification accuracies of the epileptic and normal data at different frequency bands. According to the results provided in Table 7, the highest accuracy was obtained when the EEG signals were filtered using a 1–40-Hz band-pass filter. It is important to mention here that, although different frequency bands were used, the combination of CSP + LBP + KNN still provided the highest accuracy, as seen in both tables.

C. EFFECT OF THE REDUCTION NUMBER

As mentioned in subsection 2C, the reduction number d is the number by which the channels can be reduced. Table 8 gives the average classification accuracies of the autistic versus normal data, which were filtered at 4–30 Hz, where a segment length of 50 s and different dimension values were used. It can be seen that the results were significantly affected, as the classification accuracy decreased with the decrease in the value of the reduction number. Table 9 shows the results of a similar investigation, but for the epileptic versus the normal data, which were filtered at 1–40 Hz, where a segment length of 30 s was used. It can be seen from Table 9 that, with an increase in the value of the reduction number from 2 to 22, the accuracy begins to increase to a certain value and then begins to decrease. The results in Tables 8 and 9 reveal that the optimal value of d is 16. It can be noted from both tables that the combination of CSP + LBP + KNN still provides the best results, especially at $d = 16$, with classification accuracy of 98.46% and 98.62% for normal versus autistic features and normal versus epileptic features, respectively. Therefore, and according to dimensionality reduction investigation, it was found that recorded channels (Fp1, Fp2, Fz, F3, F4, F7, F8, Cz, C3, C4, T3, T5, Pz, Oz, O1, and O2) contain important information on whether to classify autism or epilepsy. After the previous comparison of the feature extraction and classification methods as well as

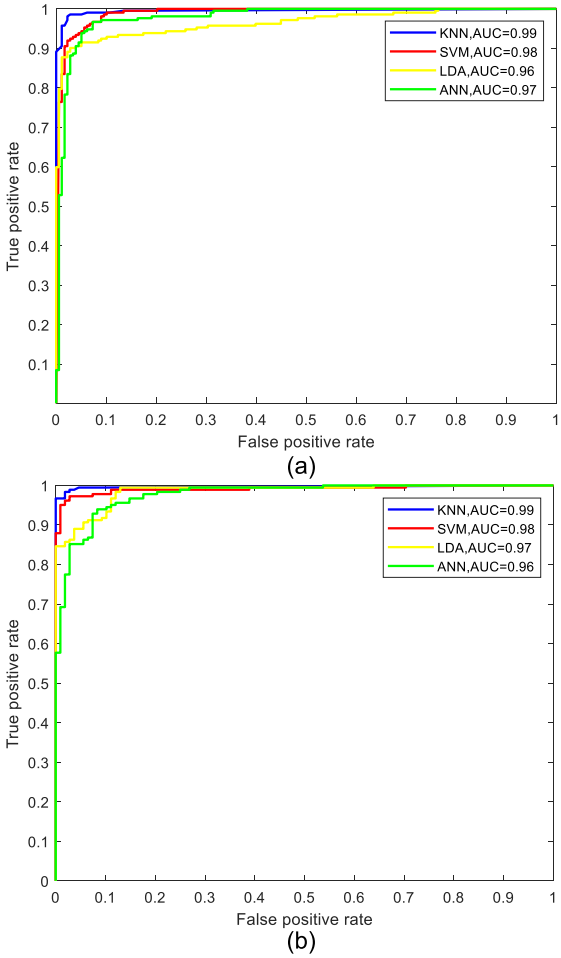

FIGURE 12. ROC-AUC of methods included in Table 10: (a) autism classification and (b) epilepsy classification.

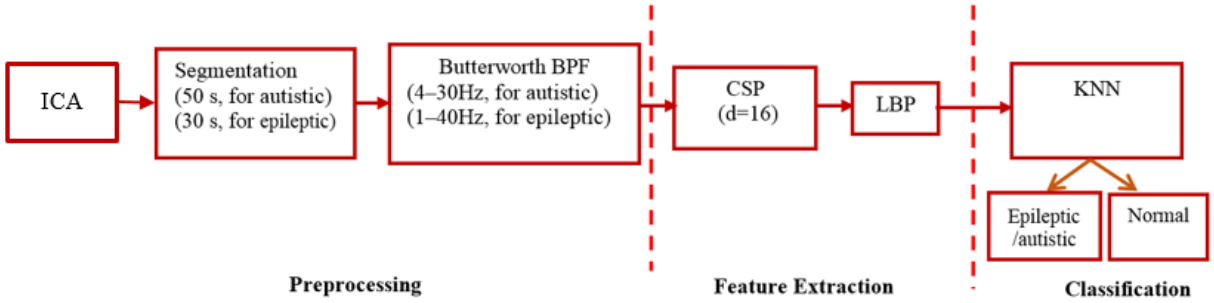

FIGURE 13. The complete method that provides the best performance.

the effects of segment length, frequency band, and reduction number, we summarize the completed methods that give the best results for the diagnosis of either autism or epilepsy. Table 10 shows the recommended method for diagnosing both autism and epilepsy with classification accuracies of 98.46% and 98.62%, respectively, with KNN classifier. Figure 12 shows ROC-AUC corresponding to these results.

Finally, the benefit of this work can be measured by comparing the results of the proposed method with the results of previous studies. Tables 11 and 12 show comparisons of our results with the results of previous works related to ASDs and epilepsy, respectively. From these tables, it can be seen that our work provides good classification accuracy compared with the previous studies.

IV. CONCLUSION AND FUTURE STUDY

In recent years, EEG signal-analysis techniques have been improved because EEG signals reflect neurological brain activities, and they have also become an important tool for diagnosing neurological brain disorders. In this study, we focused on the diagnosis of epilepsy and ASDs through the analysis and processing of EEG signals. In addition, we used new techniques for feature extraction using CSP, which has not been used in previous studies. In addition to variance, we used entropy, energy, and BP to construct the feature vector. Then, for investigation, we used four techniques for classification: LDA, SVM, KNN, and ANN. The aim of this investigation was to compare the proposed approaches and recommend the best combination for diagnosing epilepsy and autism. We also investigated the effects of segment length, filter frequency band, and reduction number on the classification accuracy. The different datasets used in this work were provided by Bonn University, Germany; MIT, USA; and King Abdulaziz University, Jeddah, Saudi Arabia, to evaluate our proposed methods.

Overall, the results showed that the features extracted using CSP and LBP resulted in the highest classification accuracy. This conclusion was confirmed by our previously reported study [40], where the CSP + LBP method was used to extract the features from motor imagery signals. In addition, the results in this study showed that the combination of CSP + LBP + KNN achieved the best results with average classification accuracy of approximately 99% for the diagnosis of both autism and epilepsy. Figure 13 shows a schematic of the complete method that achieved the best performance in comparison with the other proposed methods. The proposed method provides very promising results that are comparable to those published in previous studies.

Finally, diagnosing of neurological brain disorders are performed manually by neurologists or skilled clinicians through visual inspection of EEG signals. Therefore, the proposed system can assist medical doctors and clinicians in order to diagnose neurological brain disorder automatically.

With the proposed system, diagnosis time is saved and the diagnosis of neurological brain disorders becomes more accurate. In future work, the proposed method will be tested and evaluated with a larger database and with other neurological brain disorders such as Alzheimer's. The proposed approach will be developed to diagnose more than two neurological brain disorders at the same time (two classes or more). Deep learning approaches will be used for classification in order to improve the classification accuracy and provide a perfect classification. One of the challenges of the proposed method is hardware implementation in order to be used for real-world diagnostics. Hardware implementation (using an FPGA, for example) remains the next work to consider.

REFERENCES

[1] E. Niedermeyer and F. L. D. Silva, *Electroencephalography: Basic Principles, Clinical Applications, and Related Fields*. Philadelphia, PA, USA: Lippincott Williams Wilkins, 2004.

[2] D. J. Thurman *et al.*, "Standards for epidemiologic studies and surveillance of epilepsy," *Epilepsia*, vol. 52, pp. 2–26, Sep. 2011, doi: 10.1111/j.1528-1167.2011.03121.x.

[3] S. Noachtar and J. Rémi, "The role of EEG in epilepsy: A critical review," *Epilepsy Behav.*, vol. 15, no. 1, pp. 22–33, May 2009, doi: 10.1016/j.yebeh.2009.02.035.

[4] V. P. Nigam and D. Graupe, "A neural-network-based detection of epilepsy," *Neurolog. Res.*, vol. 26, no. 1, pp. 55–60, Jan. 2004, doi: 10.1179/016164104773026534.

[5] N. Kannathal, M. L. Choo, U. R. Acharya, and P. K. Sadasivan, "Entropies for detection of epilepsy in EEG," *Comput. Methods Programs Biomed.*, vol. 80, no. 3, pp. 187–194, Dec. 2005, doi: 10.1016/j.cmpb.2005.06.012.

[6] N. Sadati, H. R. Mohseni, and A. Maghsoudi, "Epileptic seizure detection using neural fuzzy networks," in *Proc. IEEE Int. Conf. Fuzzy Syst.*, Jul. 2006, pp. 596–600.

[7] H. Ocak, "Automatic detection of epileptic seizures in EEG using discrete wavelet transform and approximate entropy," *Expert Syst. Appl.*, vol. 36, no. 2, pp. 2027–2036, Mar. 2009, doi: 10.1016/j.eswa.2007.12.065.

[8] T. M. Nunes, A. L. V. Coelho, C. A. M. Lima, J. P. Papa, and V. H. C. D. Albuquerque, "EEG signal classification for epilepsy diagnosis via optimum path forest—A systematic assessment," *Neurocomputing*, vol. 136, pp. 103–123, Jul. 2014, doi: 10.1016/j.neucom.2014.01.020.

[9] A. Subasi and M. I. Gursoy, "EEG signal classification using PCA, ICA, LDA and support vector machines," *Expert Syst. Appl.*, vol. 37, no. 12, pp. 8659–8666, Dec. 2010, doi: 10.1016/j.eswa.2010.06.065.

[10] A. Subasi, "EEG signal classification using wavelet feature extraction and a mixture of expert model," *Expert Syst. Appl.*, vol. 32, no. 4, pp. 1084–1093, May 2007, doi: 10.1016/j.eswa.2006.02.005.

[11] M. Zhou, C. Tian, R. Cao, B. Wang, Y. Niu, T. Hu, H. Guo, and J. Xiang, "Epileptic seizure detection based on EEG signals and CNN," *Frontiers Neuroinform.*, vol. 12, p. 95, Dec. 2018, doi: 10.3389/fninf.2018.00095.

[12] M. Li, W. Chen, and T. Zhang, "Classification of epilepsy EEG signals using DWT-based envelope analysis and neural network ensemble," *Biomed. Signal Process. Control*, vol. 31, pp. 357–365, Jan. 2017, doi: 10.1016/j.bspc.2016.09.008.

[13] K. D. Tzimourta, A. T. Tzallas, N. Giannakeas, L. G. Astrakas, D. G. Tsalikakis, P. Angelidis, and M. G. Tsipouras, "A robust methodology for classification of epileptic seizures in EEG signals," *Health Technol.*, vol. 9, no. 2, pp. 135–142, Mar. 2019, doi: 10.1007/s12553-018-0265-z.

[14] X. Zhang, L. Yao, M. Dong, Z. Liu, Y. Zhang, and Y. Li, "Adversarial representation learning for robust patient-independent epileptic seizure detection," *IEEE J. Biomed. Health Inform.*, vol. 24, no. 10, pp. 2852–2859, Oct. 2020, doi: 10.1109/JBHI.2020.2971610.

[15] A. Sheikhani, H. Behnam, M. R. Mohammadi, M. Noroozian, and P. Golabi, "Connectivity analysis of quantitative electroencephalogram background activity in autism disorders with short time Fourier transform and coherence values," in *Proc. Congr. Image Signal Process.*, May 2008, pp. 207–212.

[16] A. Sheikhani, H. Behnam, M. R. Mohammadi, M. Noroozian, and M. Mohammadi, "Detection of abnormalities for diagnosing of children with autism disorders using of quantitative electroencephalography analysis," *J. Med. Syst.*, vol. 36, no. 2, pp. 957–963, Apr. 2012, doi: 10.1007/s10916-010-9560-6.

[17] M. Ahmadlou, H. Adeli, and A. Adeli, "Fractality and a wavelet-chaos-neural network methodology for EEG-based diagnosis of autistic spectrum disorder," *J. Clin. Neurophysiol.*, vol. 27, no. 5, pp. 328–333, Oct. 2010, doi: 10.1097/WNP.0b013e3181f40dc8.

[18] M. Ahmadlou, H. Adeli, and A. Adeli, "Improved visibility graph fractality with application for the diagnosis of autism spectrum disorder," *Phys. A, Stat. Mech. Appl.*, vol. 391, no. 20, pp. 4720–4726, Oct. 2012, doi: 10.1016/j.physa.2012.04.025.

[19] M. Ahmadlou, H. Adeli, and A. Adeli, "Fuzzy synchronization likelihood-wavelet methodology for diagnosis of autism spectrum disorder," *J. Neurosci. Methods*, vol. 211, no. 2, pp. 203–209, Nov. 2012, doi: 10.1016/j.jneumeth.2012.08.020.

[20] W. Bosl, A. Tierney, H. Tager-Flusberg, and C. Nelson, "EEG complexity as a biomarker for autism spectrum disorder risk," *BMC Med.*, vol. 9, no. 1, p. 18, Dec. 2011, doi: 10.1186/1741-7015-9-18.

[21] M. J. Alhaddad, M. I. Kamel, and H. M. Malibary, "Diagnosis autism by Fisher linear discriminant analysis FLDA via EEG," *Int. J. Bio-Sci. Bio-Technol.*, vol. 4, no. 2, pp. 45–54, 2012.

[22] E. A. Alsaggaf and M. I. Kamel, "Using EEGs to diagnose autism disorder by classification algorithm," *Life Sci. J.*, vol. 11, no. 6, pp. 305–308, 2014.

[23] J. Fan, J. W. Wade, D. Bian, A. P. Key, Z. E. Warren, L. C. Mion, and N. Sarkar, "A step towards EEG-based brain computer interface for autism intervention," in *Proc. 37th Annu. Int. Conf. IEEE Eng. Med. Biol. Soc. (EMBC)*, Aug. 2015, pp. 3767–3770, doi: 10.1109/EMBC.2015.7319213.

[24] H. Hadoush, M. Alafeef, and E. Abdulhay, "Automated identification for autism severity level: EEG analysis using empirical mode decomposition and second order difference plot," *Behavioural Brain Res.*, vol. 362, pp. 240–248, Apr. 2019, doi: 10.1016/j.bbr.2019.01.018.

[25] D. Abdolzadegan, M. H. Moattar, and M. Ghoshuni, "A robust method for early diagnosis of autism spectrum disorder from EEG signals based on feature selection and DBSCAN method," *Biocybernetics Biomed. Eng.*, vol. 40, no. 1, pp. 482–493, Jan. 2020, doi: 10.1016/j.bbe.2020.01.008.

[26] J. Kang, X. Han, J. Song, Z. Niu, and X. Li, "The identification of children with autism spectrum disorder by SVM approach on EEG and eye-tracking data," *Comput. Biol. Med.*, vol. 120, May 2020, Art. no. 103722, doi: 10.1016/j.compbiomed.2020.103722.

[27] A. L. Goldberger, J. M. Hausdorff, H. E. Stanley, L. A. N. Amaral, L. Glass, P. C. Ivanov, R. G. Mark, J. E. Mietus, G. B. Moody, and C.-K. Peng, "PhysioBank, PhysioToolkit, and PhysioNet: Components of a new research resource for complex physiologic signals," *Circulation*, vol. 101, no. 23, pp. E215–E220, Jun. 2000. [Online]. Available: https://archive.physionet.org/pn6/chbmit/, doi: 10.1161/01.cir.101.23.e215.

[28] A. Shoeb, "Application of machine learning to epileptic, seizure onset detection and treatment," Ph.D. dissertation, MIT, Cambridge, MA, USA, 2009.

[29] S. Ibrahim, R. Djemal, and A. Alsuwailem, "Electroencephalography (EEG) signal processing for epilepsy and autism spectrum disorder diagnosis," *Biocybernetics Biomed. Eng.*, vol. 38, no. 1, pp. 16–26, 2018, doi: 10.1016/j.bbe.2017.08.006.

[30] J. Müller-Gerking, G. Pfurtscheller, and H. Flyvbjerg, "Designing optimal spatial filters for single-trial EEG classification in a movement task," *Clin. Neurophysiol.*, vol. 110, no. 5, pp. 787–798, 1999, doi: 10.1016/s1388-2457(98)00038-8.

[31] B. Blankertz, R. Tomioka, S. Lemm, M. Kawanabe, and K.-R. Müller, "Optimizing spatial filters for robust EEG single-trial analysis," *IEEE Signal Process. Mag.*, vol. 25, no. 1, pp. 41–56, 2008, doi: 10.1109/MSP.2008.4408441.

[32] R. O. Duda, *Pattern Classification*. Hoboken, NJ, USA: Wiley, 2012.

[33] C. J. C. Burges, "A tutorial on support vector machines for pattern recognition," *Data Mining Knowl. Discovery*, vol. 2, no. 2, pp. 121–167, 1998, doi: 10.1023/A:1009715923555.

[34] K. Q. Weinberger and L. K. Saul, "Distance metric learning for large margin nearest neighbor classification," *J. Mach. Learn. Res.*, vol. 10, pp. 207–244, Feb. 2009.

[35] P. Refaeilzadeh, L. Tang, and H. Liu, "Cross-validation," in *Encyclopedia of Database Systems*, M. T. Özsu and L. Liu, Eds. Springer, 2009.

[36] T. Fawcett, "An introduction to ROC analysis," *Pattern Recognit. Lett.*, vol. 27, no. 8, pp. 861–874, Jun. 2006, doi: 10.1016/j.patrec.2005.10.010.

[37] H. Ramoser, J. Muller-Gerking, and G. Pfurtscheller, "Optimal spatial filtering of single trial EEG during imagined hand movement," *IEEE Trans. Rehabil. Eng.*, vol. 8, no. 4, pp. 441–446, Dec. 2000, doi: 10.1109/86.895946.

[38] S. G. Mason, A. Bashashati, M. Fatourechi, K. F. Navarro, and G. E. Birch, "A comprehensive survey of brain interface technology designs," *Ann. Biomed. Eng.*, vol. 35, no. 2, pp. 137–169, Jan. 2007, doi: 10.1007/s10439-006-9170-0.

[39] Y. U. Khan, N. Rafiuddin, and O. Farooq, "Automated seizure detection in scalp EEG using multiple wavelet scales," in *Proc. IEEE Int. Conf. Signal Process., Comput. Control*, Waknaghat Solan, India, Mar. 2012, pp. 1–5.

[40] M. Aljalal, R. Djemal, and S. Ibrahim, "Robot navigation using a brain computer interface based on motor imagery," *J. Med. Biol. Eng.*, vol. 39, no. 4, pp. 508–522, Aug. 2019, doi: 10.1007/s40846-018-0431-9.

FAHD A. ALTURKI received the B.S. degree in electrical engineering from King Saud University, Riyadh, Saudi Arabia, in 1986, the M.S. degree in control systems from Imperial College London, London, U.K., in 1988, and the Ph.D. degree in control engineering from The University of Sheffield, Sheffield, U.K., in 1993. From 2008 to 2012, he was the Dean of the College of Engineering and has been the General Supervisor of King Saud University colleges, Almuzahimiah Branch, since April 2013. He is currently a Professor of electrical engineering with King Saud University. His main research interests include intelligent systems, signal processing, and nonlinear control.

MAJID ALJALAL received the B.S. degree in communication engineering from Taiz University, Taiz, Yemen, in 2010, and the M.S. degree in electrical engineering from King Saud University, Riyadh, Saudi Arabia, in 2017, where he is currently pursuing the Ph.D. degree with the Department of Electrical Engineering. His research interests include artificial intelligence, brain–computer interfaces, control systems, and EEG signal processing.

AKRAM M. ABDURRAQEEB received the B.S. degree in communication and computer engineering from Taiz University, Taiz, Yemen, in 2008, and the M.S. degree in automatic control from the Department of Electrical Engineering, King Saud University, Riyadh, Saudi Arabia, in 2017. He is currently pursuing the Ph.D. degree in automatic control with the Department of Electrical Engineering. His research interests include application of robust control for micro/nano-positioning systems, artificial intelligence, robotics, and EEG signal processing.

KHALIL ALSHARABI was born in Taiz, Yemen, in 1983. He received the B.S. degree in communication and computer engineering from Taiz University, Yemen, in 2008, and the M.S. degree in electrical engineering and in control systems engineering from King Saud University, Saudi Arabia, in 2017, where he is currently pursuing the Ph.D. degree with the Department of Electrical Engineering. His research interests include brain–computer interfaces, EEG signal processing, control systems engineering, and artificial intelligence.

ABDULLRAHMAN A. AL-SHAMMA'A was born in Sana'a, Yemen, in 1984. He received the bachelor's degree in electrical engineering and in electrical power and machines from Sana'a University, Sana'a, in 2008, and the M.Sc. and Ph.D. degrees from King Saud University, Riyadh, Saudi Arabia, in 2013 and 2019, respectively, both in electrical engineering. In 2019, he joined King Saud University, where he is currently an Adjunct Assistant Professor with the Department of Electrical Engineering. He has published many research articles in peer-reviewed journals, in addition to many international conference papers. In the field of multilevel converters, he received two patents for simple and efficient power converters, including applications to grid-connected photovoltaic plants. His research interests include the design, control, and optimization of renewable energy systems, as well as multilevel power electronics converters for micro-grids and electric drive applications.